ChemPubSoc Europe

DOI: 10.1002/slct.201900561

Chemistry SELECT Full Papers

Materials Science inc. Nanomaterials & Polymers

Zn(II) Di-isobutyldithiocarbamate Complex Enabled Efficient Synthesis of Au/ZnS Nanocomposite Core-shell in One Pot

Rathindranath Biswas, Harjinder Singh, Biplab Banerjee, and Krishna K. Haldar*[a]

Here, we demonstrate a one pot synthesis of gold/zinc sulphide (Au/ZnS) core-shell type composite nanostructure via thermal decomposition of single molecular precursor Zn(II)di-isobutyldithiocarbamate complex. In these Au/ZnS core-shell type hybrid nanostructures where ZnS quantum dots are assembled onto Au nanoparticles surface were prepared via a facile and reproducible approach under mild conditions. The crystalline nature and interface of these Au/ZnS core-shell type composite nanostructures were confirmed by X-ray powder diffraction (XRD), X-ray photoelectron spectroscopy (XPS), High-resolution transmission electron microscopy (HRTEM) and inverted TEM images. Here Zn(II)di-isobutyldithiocarbamate complex acts as ZnS source as well as reducing and stabilizing agent for Au^0 at their nanoscale range by coating in the reaction medium.

Introduction

The nanocomposites consisting of noble metallic[1] and transition metal chalcogenide[2] (TMC) nanomaterials are promising for scientific research due to plasmon-exciton interaction.[3] Such multifunctional nanomaterials have attracted great interest in last few years due to their distinctive physical as well as chemical properties which lead to admirable performance in electronic,[4] magnetic,[5] photocatalytic,[6] optoelectronic[7] and biological applications[8] over their constituent materials. A wide diversity of metal- TMC based hybrid nanostructures such as core-shell,[9] tetrapod,[10] pentapod,[11] nanoflower,[12] dumbbells[13] etc are reported. Among these hybrid structures, metal/ TMC core-shell nanocrystals have paid considerable attention for efficient photogenerated carriers for various photoinduced applications.[14] Among them, gold (Au)/zinc sulphide (ZnS) hybrid materials are widely used as the metal/ TMC composite nanocrystals till date due to its complementary optoelectronic properties arising from their nanoscale constituents. Probably ZnS is the most important materials practiced as phosphor host.[15] Hsu *et. al* reported a L-cysteine-assisted Au/ZnS core/shell nanocrystals formation via hydrothermal approach for methanol oxidation.[16] Recently, Yang group fabricated ternary Au/MnS/ZnS Core/Shell/Shell nanocomposite and uses it for magnetic resonance imaging and enhanced cancer radiation therapy application.[17] Yu *et.al* demonstrated the designing of Au loaded ZnS nanoflowers and applied this for hydrogen production during photocatalytic process.[18] However, synthesis of these hybrid Au/ZnS core-shell nanostructures is not unequivocal in the manner that Au or ZnS nanocrystals form; whereas, it demands a more choosy approach to carry both their counterparts together. For illustration, in most of the cases these hybrid Au/ZnS core-shell nanostructures were achieved by growing ZnS parts on a preformed Au nanoparticle via the colloidal/thermal deposition route.[16] Briefing the results from literature, we noticed that Au/ZnS core-shell hybrid nanostructures were mostly prepared by colloidal based technique. However, the designing of such core-shell nanostructures remains complicated for the synchronous nucleation and growth of the ZnS nanocrystals shell on Au nanoparticles periphery which require a high-temperature reaction system. To the best of our knowledge, there is no report till date on the fabrication of Au/ZnS core-shell type hybrid nanostructure synthesized in one pot using Zn(II)di-isobutyldithiocarbamate complex molecular precursor via a colloidal process. Here, Au/ZnS core-shell type hybrid nanostructure i.e. ZnS quantum dots assembled onto Au nanoparticles surface were synthesized via a facile and reproducible approach under mild conditions.

In this work, we have fabricated ZnS quantum dots assembled on Au nanoparticles surface leading to a Au/ZnS core-shell type composite nanostructure in one pot employing thermal decomposition of single molecular precursor Zn(II)di-isobutyldithiocarbamate complex. Here Zn(II)di-isobutyldithiocarbamate complex functioned as ZnS source as well as reducing and stabilizing agent for Au^0 at nanoscale by coating in the reaction medium.

Results and Discussion

ZnS QDs stabilized Au nanoparticles composite structures i.e. Au/ZnS core-shell structures were synthesized in non-aqueous solution using a thermal decomposition reaction of Zn (II) di-isobutyldithiocarbamate complex in presence of $HAuCl_4$. Both ZnS QDs and Au NPs have inherent optical property. Figure 1 presents the absorbance spectra of ZnS in absence and

[a] *R. Biswas, H. Singh, Dr. B. Banerjee, Dr. K. K. Haldar*
Department of Chemical Sciences, School of Basic and Applied Sciences, Central University of Punjab, Bathinda, 151001, Punjab, India
E-mail: cskkh@cup.ac.in

Supporting information for this article is available on the WWW under https://doi.org/10.1002/slct.201900561

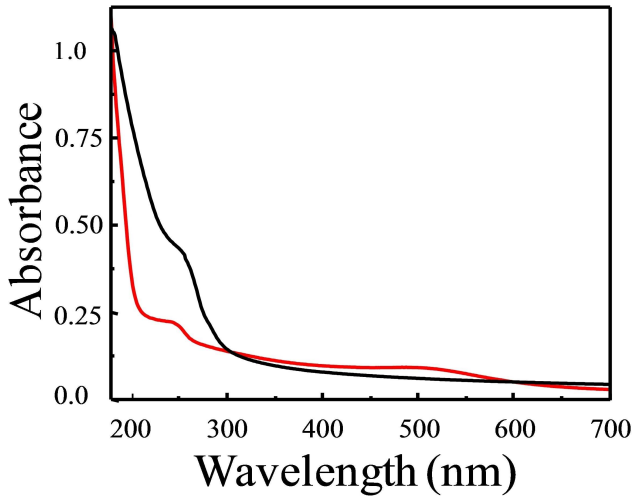

Figure 1. Absorbance spectra of (a) Pure ZnS QDs (Black), and (b) Au/ZnS (Red) composite core shell nanocrystals.

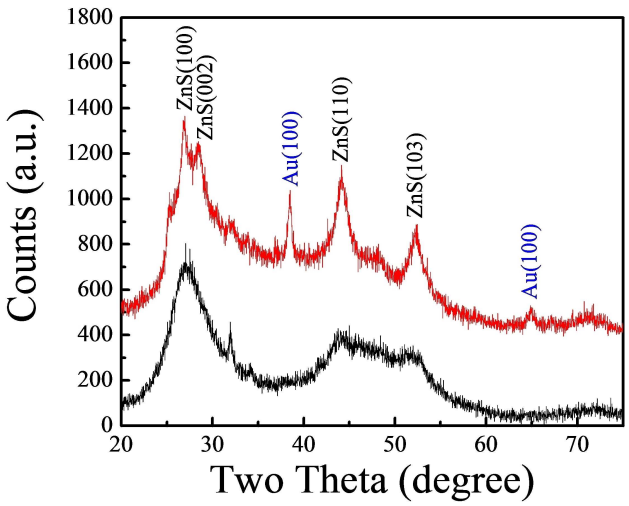

Figure 2. The XRD pattern of as-prepared (a) ZnS QDs (Black) and (b) Au/ZnS (Red) composite core-shell nanocrystals.

presence of Au nanoparticles. The peak appeared at 276 nm is due to pure ZnS QDs (fig 1a). Again, this band position in Au/ZnS core-shell nanostructure is blue shifting from 276 nm to 249 nm which is obviously due to the shell of ZnS on Au nanoparticles. In addition, the existence of red shifted and broad surface plasmon is due to coupling with the exciton of ZnS, band centered at 524 nm which indicates the presence of Au in the Au/ZnS composite nanostructure (fig 1b).[19] This observation clearly demonstrates the formation of ZnS QDs stabilized Au nanoparticles composite Au/ZnS core-shell type nanostructure. And it also implies that the absorption in the visible region is slightly higher in ZnS/Au core-shell nanoparticle when compared to that of ZnS nanoparticles which is due to surface plosmon effect of Au. Therefore, presence of Au in the Au/ZnS core-shell nanostructure can lead to faster separation of the photogenerated charge carriers and thus improve the light-absorption efficiency of ZnS.[18]

Again, to know the crystalline nature of the as formed Au/ZnS composite core-shell type nanostructure, we have investigated the powder X-ray diffraction (XRD) patterns of Au/ZnS composite nanocrystals and ZnS QDs. Figure 2 depicts the powder X-ray diffraction (XRD) patterns of Au/ZnS composite nanocrystals. XRD pattern (fig.2a) reveals three broad peaks at two theta (2θ) values of 26.9°, 45.1° and 52.3° corresponding to the plane (100), (110) and (103) of hexagonal ZnS, respectively. The broad peaks indicate that the as prepared ZnS are very small and well crystalline in nature. However, in Au/ZnS composite core-shell nanostructure all the major peaks of ZnS at 26.9°, 28.4°, 45.1° and 52.3° were indexed for (100), (002), (110) and (103) planes along with two additional peaks for Au at 38.1° and 64.2° for (111) and (003) planes (fig.2b). It is believed that the relatively small quantity of Au in compared to ZnS and surrounded by ZnS are responsible for its lower intensity in the XRD spectra. So the appearance of two strong peaks at 38.1° and 64.2° clearly confirms the presence of face centred cubic Au in the Au/ZnS hybrid nanostructure and results the formation of Au/ZnS composite core-shell nanostructure. In addition, no other crystalline impurities or no remarkable diffraction peak shifting were observed.

Finally, after the formation of Au/ZnS composite core-shell nanostructure and the interface between Au and ZnS, we have studied the transmission electron microscope (TEM) and high resolution TEM images of the as prepared Au/ZnS core-shell nanostructure and pure ZnS QDs. Figure 3a demonstrated TEM

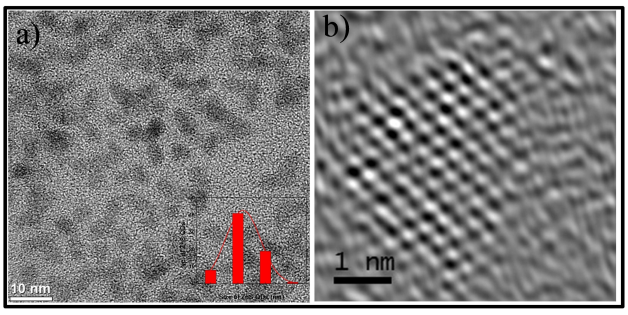

Figure 3. (a) TEM images of ZnS QDs (the inset picture represents the corresponding distribution graph of ZnS QDs) and (b) inverse FFT of a single ZnS QDs.

images of the pure ZnS QDs which was produced in absence of Au-TOAB precursor in the similar reaction. The TEM images clearly demonstrated that pure ZnS QDs are well crystalline with good monodispersity. The inset picture of figure 3a shows the corresponding particles distribution of ZnS QDs which indicates that ZnS have almost equal sizes with average sizes of 3.2 ± 0.1 nm and well lattice fringe (Fig. 3b). Figure 4 shows the typical TEM images of the as prepared Au/ZnS composite core-shell nanostructure. Without size sorting, the Au/ZnS multifunctional nanocrystals captured here displays almost homodispersity. The Au/ZnS core-shell composite structures possess a

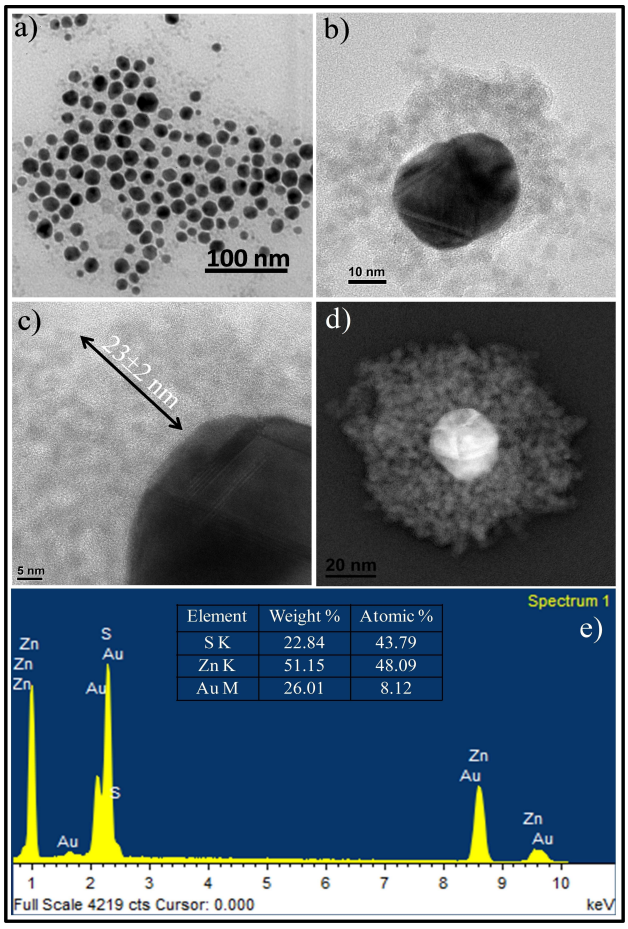

Figure 4. (a) Wide view TEM images of Au/ZnS composite nanostructures (b) and (c) Typical HRTEM images of a single Au/ZnS composite nanostructures showing Au in the core, and ZnS QDs are decorated on the surface. Figure (d) represents the inverted TEM images a single Au/ZnS composite nanostructure. (e) Shows the corresponding EDS data of Au/ZnS core-shell nanostructures.

highly crystalline structure, which is continual with the X-ray diffraction data. Wide view TEM images of the nanocrystals clearly show that almost all the Au nanoparticles are coated with a thick layer of ZnS (fig.4a). This is because of the presence of ZnS QDs at that periphery of Au nanoparticles where ZnS QDs act as a protective stabilizing agent towards the aggregation of Au nanoparticles. Overall, the ZnS QDs in all the nanocomposite structures of Au/ZnS are uniform in morphology. In addition, the TEM images of higher magnification affirm that the diameter of the as formed ZnS QDs shell about ~23± 2 nm (figure 4b & c). Again, to confirm the deposition of ZnS QDs on the Au surface to form a thick shell of ZnS, we have taken the inverted HRTEM images. The inverted HRTEM images (fig. 4d) have clearly demonstrated that the as synthesized ZnS QDs assembled on the preformed Au giving rise to a three dimensional Au/ZnS core-shell nanocomposite structure. Additionally, the chemical composition of Au/ZnS core-shell nanostructure was investigated by energy dispersive spectroscopy (EDS). The EDS patern (figure 4e) clearly verifies the presence of the elements Au, Zn, and S (as shown in the table insert in the figure 4e) in the Au/ZnS core-shell nanocomposite. The results of EDS analysis reveal that the Au/ZnS core–shell nanocrystals have a high purity and the ratios (atomic) were found to be 43.79% S, 48.09% Zn and 8.12% Au.

To further investigate the chemical composition of Au/ZnS composite core-shell nanostructures, we have carried out X-ray photoelectron spectroscopy (XPS) measurements. Figure 5

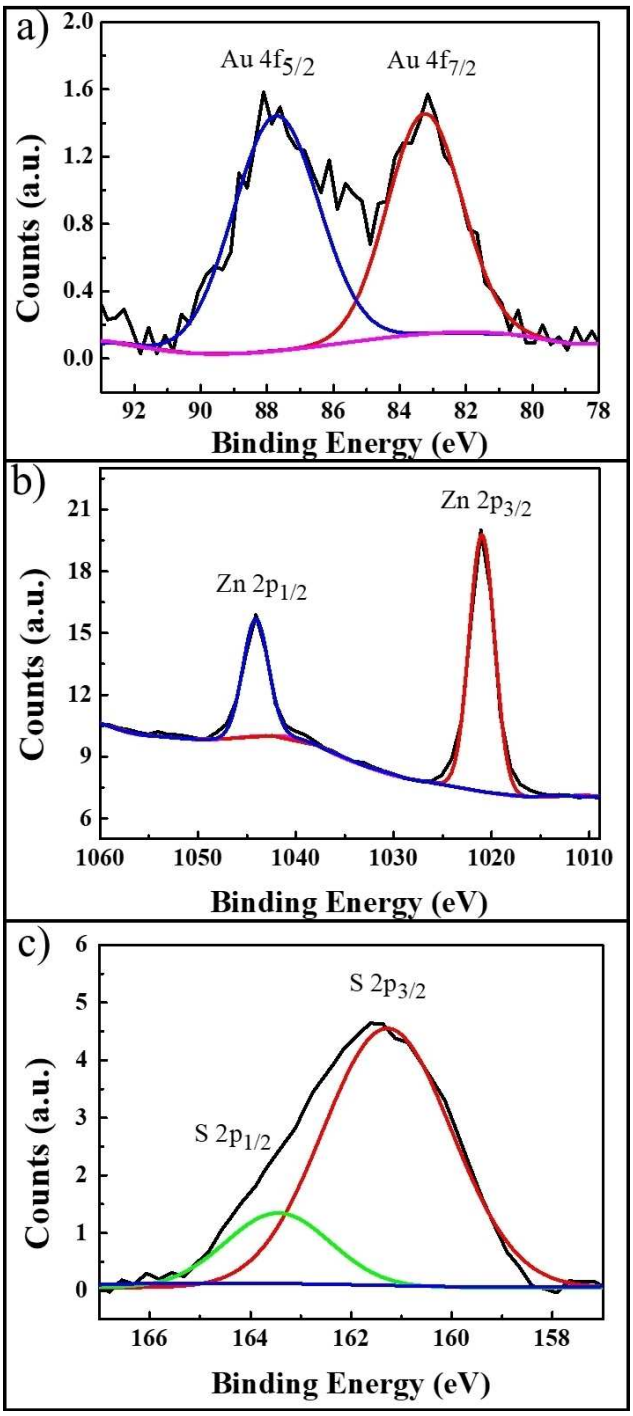

Figure 5. XPS spectra of (a) Au 4f and (b) Zn 2p and (c) S 2p in Au/ZnS composite core-shell nanostructures.

shows the XPS spectra of Au, Zn, and S. The photoemission spectra of Au appear at the binding energy values of 83.2 eV and 87.7 eV (fig. 5 panel a) due to 4f 7/2 and 4d 5/2 peaks, respectively, and no peak was observed at 84.9 eV for Au^{+}. This result suggested that Au atoms exist in metallic state in this Au/ZnS composite nanostructure.[20] Again, compared to the bulk gold materials, the slight shifting of Au 4f7/2 peak in Au/ZnS core-shell is attributed to the changes in the electronic structure due to the appearance of charge transfer among Au and ZnS.[14,21] Notably, all samples show two strong peaks at the binding energy values of 1021 and 1044.1 eV attributed to Zn 2p3/2 and Zn 2p1/2, respectively, which indicate that Zn is in Zn^{2+} (fig. 5 panel b) form.[22] In the fig. 5 panel c, the photoemission peak of S spectrum was deconvoluted into two components by Gaussian fitting, which can be assigned to the spin-orbit splitting to S(2p). The peaks centred at the binding energy of 161.2 and 163.5 eV are assigned to S 2p3/2 and S 2p1/2 core levels of S^{2-} anions, respectively present in ZnS of Au/ZnS composite nanostructure.[23]

In order to rationalize the formation of composite Au/ZnS core-shell nanoparticles from the molecular Zn (II) di-isobutyldithiocarbamate complex in presence of $HAuCl_4$, we have investigated the fabrication process via FT-IR and ATR-FTIR studies of the Zn (II) di-isobutyldithiocarbamate complex and Au/ZnS composite nanocrystals. Figure 6 (panel a) shows the FTIR spectra of as synthesized Zn (II) di-isobutyldithiocarbamate complex. The peaks at 2978 cm^{-1} and 2869 cm^{-1} are due to the asymmetric and symmetric stretching vibration of $-CH_3$, respectively.[24] The C–N vibration bands were observed at 1383 cm^{-1}, 1178 cm^{-1} and 1093 cm^{-1}.[25] Peaks at 993 cm^{-1}, 968 cm^{-1} and 881 cm^{-1} may be attributed to the C=S in the $-CSS^{-}$ group.[26] However, the band corresponding to the C–S vibration was observed around 748 cm^{-1}, 695 cm^{-1}, 658 cm^{-1}. The formation of the Zn(II) di-isobutyldithiocarbamate complex was further confirmed by the characteristic peaks appeared at 580 cm^{-1}, 486 cm^{-1}, 466 cm^{-1} and 445 cm^{-1} which are attributed to the stretching vibration of Zn–S bond.[26] Both the formation of Zn (II) di-isobutyldithiocarbamate complex and the mechanism of the fabrication of core- shell Au/ZnS nanostructure was further confirmed by the ATR-IR Spectroscopy study (fig. 6 panel b). Two strong peaks at 584 cm^{-1} and 556 cm^{-1} along with two weak peaks at 456 cm^{-1} and 437 cm^{-1} were observed which corresponded to the stretching vibration of Zn–S. The peaks at 316 cm^{-1}, 287 cm^{-1}, 270 cm^{-1} and 221 cm^{-1} resemble the Au–S stretching vibrational modes.[27] These peaks are endorsed to the formation of Au/ZnS core-shell nanocomposites. From these FT-IR and ATR-FTIR investigation studies, it is believed that atfirst Au nanoparticles were formed. Then ZnS QDs which was produced by heating of the Zn(II) di-isobutyldithiocarbamate complex, was decorated on the surface of the Au to form Au/ZnS composite nanostructures. Since sulfur (S) is a soft donating atom and Au is also soft, the stronger affinity of Au towards softer sulfur donor make strong interaction[28] (soft-soft interaction between Au and S) of ZnS QDs and Au nanoparticles, facilitating the formation of Au/ZnS composite nanostructures.

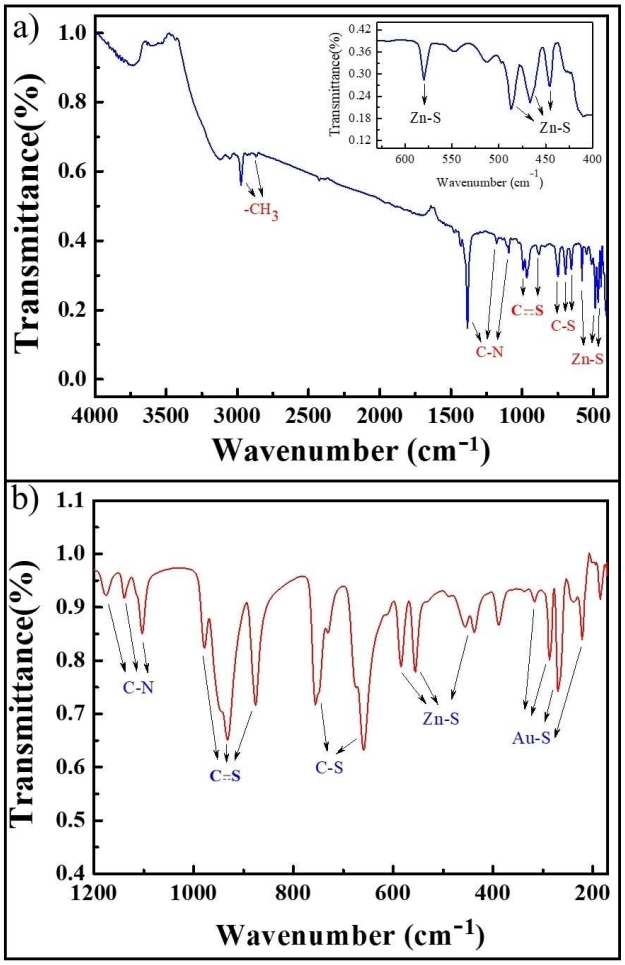

Figure 6. (a) FTIR spectra of synthesized Zn (II) di-isobutyldithiocarbamate complex, (b) ATR-FTIR Au/ZnS composite core-shell nanostructures.

Conclusion

Here we have efficiently synthesized Au/ZnS core-shell type composite nanostructure in one pot via the thermal decomposition of single molecular precursor Zn(II) di-isobutyldithiocarbamate complex. Thus we have developed a method to synthesize large scale monodisperse Au/ZnS core-shell type bybrid nanostructure. The interface between gold and zinc sulphide were investigated and found to be epitaxial. In the Au/ZnS core-shell type hybrid nanostructure, Zn (II) di-isobutyldithiocarbamate complex functioned as source of ZnS QDs and also stabilizer of Au. It is believed that due to the strong soft-soft interaction between Au nanoparticles and S of ZnS QDs facilitated the formation of Au/ZnS composite nanostructures. Such new synthetic strategy for obtaining hetero-epitaxy for metal/ TMC of hybrid nanostructures may open up new opportunities for the development of high-performance photocatalysts.

Supporting information summary

Details experimental procedure and instruments used for the characterization of Au/ZnS core-shell type composite nanostructure are available in supporting information.

Acknowledgements

This work was financially supported by the Department of Science and Technology, DST (Project No. EEQ/2017/000467) is gratefully acknowledged. We also acknowledge IACS for providing the UHR-FEG-TEM and XPS facilities. The paper was written through contributions of all authors. All authors have given approval to the final version of the paper.

Conflict of Interest

The authors declare no conflict of interest.

Keywords: Au/ZnS · Complex · Core-shell nanostructure · One-pot · Zn(II) Di-isobutyldithiocarbamate.

[1] a) C. Noguez, *J. Phys. Chem. C* **2007**, *111*, 3806–3819; b) V. Garg, B. S. Sengar, A. Kumar, G. Siddharth, S. Kumar, S. Mukherjee, *Solar Energy* **2019**, *178*, 114–124; c) R. G. Hobbs, V. R. Manfrinato, Y. Yang, S. A. Goodman, L. Zhang, E. A. Stach, K. K. Berggren, *Nano lett.* **2016**, *16*, 4149–4157; d) I. O. Sosa, C. Noguez, R. G. Barrera, *J. Phys. Chem. B* **2003**, *107*, 6269–6275; e) V. Garg, B. S. Sengar, V. Awasthi, A. Kumar, R. Singh, S. Kumar, C. Mukherjee, V. Atuchin, S. Mukherjee, *ACS Appl. Mater. Interfaces.* **2018**, *10*, 5464–5474; f) W. Rechberger, A. Hohenau, A. Leitner, J. Krenn, B. Lamprecht, F. Aussenegg, *Opt. Commun.* **2003**, *220*, 137–141; g) V. Garg, B. S. Sengar, V. Awasthi, P. Sharma, C. Mukherjee, S. Kumar, S. Mukherjee, *RSC Adv.* **2016**, *6*, 26216–26226.

[2] a) P. Jiang, Z. Q. Tian, C. N. Zhu, Z. L. Zhang, D. W. Pang, *Chem. Mater.* **2011**, *24*, 3–5; b) D. Xu, Y. Xu, D. Chen, G. Guo, L. Gui, Y. Tang, *Adv. Mater.* **2000**, *12*, 520–522; c) L. Qu, X. Peng, *J. Am. Chem. Soc.* **2002**, *124*, 2049–2055; d) D. C. Look, *Mater. Sci. Eng., B* **2001**, *80*, 383–387; e) C. Soci, A. Zhang, B. Xiang, S. A. Dayeh, D. Aplin, J. Park, X. Bao, Y.-H. Lo, D. Wang, *Nano lett.* **2007**, *7*, 1003–1009; f) X. Fang, T. Zhai, U. K. Gautam, L. Li, L. Wu, Y. Bando, D. Golberg, *Prog. Mater. Sci.* **2011**, *56*, 175–287; g) C. Ma, D. Moore, J. Li, Z. L. Wang, *Adv. Mater.* **2003**, *15*, 228–231.

[3] a) D. Zheng, S. Zhang, Q. Deng, M. Kang, P. Nordlander, H. Xu, *Nano lett.* **2017**, *17*, 3809–3814; b) W. Liu, B. Lee, C. H. Naylor, H.-S. Ee, J. Park, A. C. Johnson, R. Agarwal, *Nano lett.* **2016**, *16*, 1262–1269; c) S. Wang, S. Li, T. Chervy, A. Shalabney, S. Azzini, E. Orgiu, J. A. Hutchison, C. Genet, P. Samorì, T. W. Ebbesen, *Nano lett.* **2016**, *16*, 4368–4374; d) J. Lee, A. O. Govorov, J. Dulka, N. A. Kotov, *Nano Lett.* **2004**, *4*, 2323–2330; e) A. O. Govorov, G. W. Bryant, W. Zhang, T. Skeini, J. Lee, N. A. Kotov, J. M. Slocik, R. R. Naik, *Nano lett.* **2006**, *6*, 984–994; f) M. Achermann, *J. Phys. Chem. Lett* **2010**, *1*, 2837–2843.

[4] V. K. Narasimhan, T. M. Hymel, R. A. Lai, Y. Cui, *ACS Nano* **2015**, *9*, 10590–10597.

[5] a) M. Casavola, V. Grillo, E. Carlino, C. Giannini, F. Gozzo, E. Fernandez Pinel, M. A. Garcia, L. Manna, R. Cingolani, P. D. Cozzoli, *Nano Lett.* **2007**, *7*, 1386–1395; b) D. Zeng, Y. Chen, Z. Wang, J. Wang, Q. Xie, D.-L. Peng, *Nanoscale* **2015**, *7*, 11371–11378.

[6] a) Y. Chen, D. Zeng, M. B. Cortie, A. Dowd, H. Guo, J. Wang, D. L. Peng, *Small* **2015**, *11*, 1460–1469; b) S. T. Kochuveedu, Y. H. Jang, D. H. Kim, *Chem. Soc. Rev.* **2013**, *42*, 8467–8493; cA. Dawson, P. V. Kamat, *J. Phys. Chem. B.* **2001**, *105*, 960–966.

[7] V. Sreeramulu, K. K. Haldar, A. Patra, D. N. Rao, *J. Phys. Chem. C.* **2014**, *118*, 30333–30341.

[8] B. Ghaemi, E. Shaabani, R. Najafi-Taher, S. Jafari Nodooshan, A. Sadeghpour, S. Kharrazi, A. Amani, *ACS Appl. Mater. Interfaces* **2018**, *10*, 24370–24381.

[9] P. Guardia, K. Korobchevskaya, A. Casu, A. Genovese, L. Manna, A. Comin, *ACS Nano* **2013**, *7*, 1045–1053.

[10] a) K. K. Haldar, V. Y. Muley, S. Datar, A. Patra, *Gold Bull.* **2017**, *50*, 105–110; b) A. Figuerola, M. v. Huis, M. Zanella, A. Genovese, S. Marras, A. Falqui, H. W. Zandbergen, R. Cingolani, L. Manna, *Nano Lett.* **2010**, *10*, 3028–3036.

[11] K. K. Haldar, G. Sinha, J. Lahtinen, A. Patra, *ACS Appl. Mater. Interfaces* **2012**, *4*, 6266–6272.

[12] a) K. K. Haldar, N. Pradhan, A. Patra, *Small* **2013**, *9*, 3424–3432; b) K. K. Haldar, R. Biswas, A. Patra, K. K. Halder, T. Sen, *Gold Bull.* **2018**, 1–7; c) K. M. AbouZeid, M. B. Mohamed, M. S. El Shall, *Small* **2011**, *7*, 3299–3307.

[13] T. Mokari, E. Rothenberg, I. Popov, R. Costi, U. Banin, *Science* **2004**, *304*, 1787–1790.

[14] T. T. Yang, W. T. Chen, Y. J. Hsu, K. H. Wei, T. Y. Lin, T. W. Lin, *J. Phys. Chem. C* **2010**, *114*, 11414–11420.

[15] R. Chen, D. J. Lockwood, *J. Electrochem. Soc* **2002**, *149*, S69-S78.

[16] W. T. Chen, Y. K. Lin, T. T. Yang, Y. C. Pu, Y. J. Hsu, *Chem. Comm.* **2013**, *49*, 8486–8488.

[17] M. Li, Q. Zhao, X. Yi, X. Zhong, G. Song, Z. Chai, Z. Liu, K. Yang, *ACS Appl. Mater. Interfaces* **2016**, *8*, 9557–9564.

[18] J. Zhang, Y. Wang, J. Zhang, Z. Lin, F. Huang, J. Yu, *ACS Appl. Mater. Interfaces* **2013**, *5*, 1031–1037.

[19] a) K. K. Haldar, T. Sen, S. Mandal, A. Patra, *ChemPhysChem* **2012**, *13*, 3989–3996; b) K. K. Haldar, T. Sen, A. Patra, *J. Phys. Chem. C.* **2008**, *112*, 11650–11656.

[20] a) G. Ertas, U. K. Demirok, S. Suzer, *Appl. Surf. Sci.* **2005**, *249*, 12–15; b) K. K. Haldar, R. Biswas, S. Tanwar, T. Sen, J. Lahtinen, *ChemistrySelect* **2018**, *3*, 7882–7890; c) Y.-F. Zhu, J. Zhang, L. Xu, Y. Guo, X. P. Wang, R.-G. Du, C. J. Lin, *Phys. Chem. Chem. Phys.* **2013**, *15*, 4041–4048.

[21] K. Yu, Z. Wu, Q. Zhao, B. Li, Y. Xie, *J. Phys. Chem. C* **2008**, *112*, 2244–2247.

[22] a) S. H. Hwang, J. Song, Y. Jung, O. Y. Kweon, H. Song, J. Jang, *Chem. Comm.* **2011**, *47*, 9164–9166; b) Y. I. Choi, S. Lee, S. K. Kim, Y. I. Kim, D. W. Cho, M. M. Khan, Y. Sohn, *J. Alloys Compd.* **2016**, *675*, 46–56.

[23] J. Cao, Q. Liu, D. Han, S. Yang, J. Yang, T. Wang, H. Niu, *RSC Adv.* **2014**, *4*, 30798–30806.

[24] a) R. Georgekutty, M. K. Seery, S. C. Pillai, *J. Phys. Chem. C.* **2008**, *112*, 13563–13570; b) S. Bhattacharyya, A. Gedanken, *J. Phys. Chem. C.* **2008**, *112*, 659–665.

[25] Y.-P. Tian, C. Y. Duan, Z. L. Lu, X. Z. You, H. K. Fun, B. C. Yip, *Polyhedron* **1996**, *15*, 1495–1502.

[26] L. N. Liu, J. G. Dai, T. J. Zhao, S. Y. Guo, D. S. Hou, P. Zhang, J. Shang, S. Wang, S. Han, *RSC Adv.* **2017**, *7*, 35075–35085.

[27] a) I. Dolamic, B. Varnholt, T. Bürgi, *Phys. Chem. Chem. Phys.* **2013**, *15*, 19561–19565; b) B. Varnholt, P. Oulevey, S. Luber, C. Kumara, A. Dass, T. Bürgi, *J. Phys. Chem. C.* **2014**, *118*, 9604–9611.

[28] F. Tielens, E. Santos, *J. Phys. Chem. C.* **2010**, *114*, 9444–9452.

Submitted: February 11, 2019
Accepted: March 26, 2019